Simulating Compact Quantum Electrodynamics with Ultracold Atoms: Probing Confinement and Nonperturbative Effects

Erez Zohar,[1] J. Ignacio Cirac,[2] and Benni Reznik[1]

[1]*School of Physics and Astronomy, Raymond and Beverly Sackler Faculty of Exact Sciences, Tel-Aviv University, Tel-Aviv 69978, Israel*

[2]*Max-Planck-Institut für Quantenoptik, Hans-Kopfermann-Strasse 1, 85748 Garching, Germany*

(Received 1 May 2012; revised manuscript received 2 July 2012; published 19 September 2012)

Recently, there has been much interest in simulating quantum field theory effects of matter and gauge fields. In a recent work, a method for simulating compact quantum electrodynamics (CQED) using Bose-Einstein condensates has been suggested. We suggest an alternative approach, which relies on single atoms in an optical lattice, carrying $2l + 1$ internal levels, which converges rapidly to CQED as l increases. That enables the simulation of CQED in $2 + 1$ dimensions in both the weak and the strong coupling regimes, hence, allowing us to probe confinement as well as other nonperturbative effects of the theory. We provide an explicit construction for the case $l = 1$ which is sufficient for simulating the effect of confinement between two external static charges.

DOI: 10.1103/PhysRevLett.109.125302 PACS numbers: 67.85.Hj, 11.15.Ha

Dynamic gauge theories are at the core of the standard model of particle physics, playing the role of the force carriers among the matter fields, and therefore are of particular significance. It was shown, using lattice gauge models and other methods, that such gauge theories exhibit the peculiar phenomenon of confinement of charges which is related to nonperturbative effects due to nonlinear interactions in the theory [1–3]. Such lattice gauge theories are believed to have a nontrivial phase structure. The simplest such theory is compact quantum electrodynamics (CQED)—a U(1) lattice gauge theory, which is believed to manifest, in $3 + 1$ dimensions, a phase transition between the confining phase (for large coupling constant g) and the nonconfining Coulomb phase (for small coupling), while in $2 + 1$ dimensions it was shown that the theory confines also in the weak coupling regime because of nonperturbative effects [1–6]. In non-Abelian Yang-Mills theories, it is believed that confinement holds for all values of the coupling constants.

Recently there has been much interest in quantum simulations of quantum field theories by utilizing methods in ultracold atoms and other systems [7]. Models have been suggested for simulating dynamical matter fields [8–10], and exotic phenomena manifested by such fields have been discussed [11–13]. However, less progress has been achieved for dynamic Abelian and non-Abelian gauge theories. Dynamic gauge theories involving spin-half states have been discussed in Refs. [14,15]. Because the electric fields in such models can obtain only two values, such models are unable to manifest the effect of electric flux tubes (but rather of different "strings"). Coloumb phase simulations have been suggested with molecular states [16], and Bose-Einstein condensates (BECs) in optical lattices [17].

In a recent work [18], we have obtained, using BECs in an optical lattice, an effective theory of a dynamic U(1) gauge theory, manifesting confinement of external static charges, with observable electric flux tubes. In this Letter, we suggest an alternative approach for simulating gauge theories in terms of a spin-gauge (SG) Hamiltonian H_l [defined in Eq. (1)], which describes interacting single atoms with internal levels playing the role of angular momentum multiplet $-l \leq m \leq l$, instead of BECs as [18]. We will show that for large values of l the SG Hamiltonian rapidly converges to the standard Abelian Kogut-Susskind model [2,19] of CQED for both the weak and strong coupling regimes. Hence, this model is able to simulate the effect of confinement as well as nonperturbative effects in the weak coupling regime, which give rise to it in $2 + 1$ dimensions. As a first step in realizing the models H_l we shall propose a method for constructing the case $l = 1$ which is sufficient for observing the effect of confinement of static charges in the strong regime. First, using the methods of Ref. [20], we construct an effective "generalized XXZ" model. Then, adapting the ideas of Ref. [18], the gauge invariance is introduced to the system with a second effective calculation. The single atoms implementation might be easier experimentally than the BEC approach, as it does not rely on the overlaps of local single-particle wave functions and thus the energy scales in the Hamiltonian may be larger. Moreover, only three atomic species are required, and they can populate every link, unlike in the BEC model.

Let us consider a 2D square lattice with single atoms which carry $2l + 1$ internal states, located on the links and described by the SG Hamiltonian:

$$H_l = \frac{g^2}{2}\sum_{\mathbf{n},k}(L^k_{z\mathbf{n}})^2 - \frac{1}{2g^2[l(l+1)]^2}\sum_{\mathbf{n}}(L^1_{+,\mathbf{n}}L^2_{+,\mathbf{n}+\hat{\mathbf{1}}}L^1_{-,\mathbf{n}+\hat{\mathbf{2}}}L^2_{-,\mathbf{n}} + \text{H.c.}), \tag{1}$$

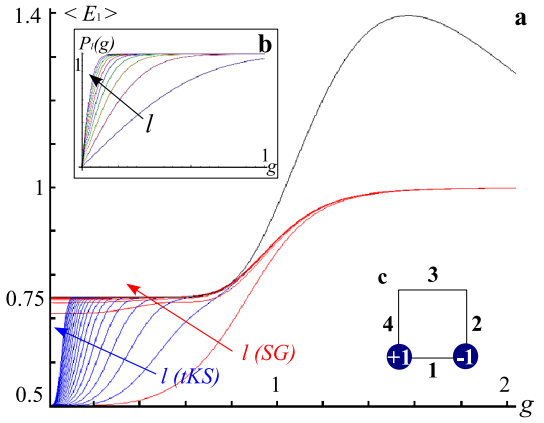

FIG. 1 (color online). Single plaquette plots. (a) Graphs of $\langle E_1(g)\rangle$. Black—the calculation of Ref. [5]—small coupling approximation for regular Abelian Kogut-Susskind theory. Blue—exact calculation for the truncated theory (tKS), for $l = 1, \ldots, 20$. Red—exact calculation for the spin-gauge theory (SG), for $l = 1, \ldots, 20$. It can be seen that the curves start to merge for a small g and l. The value 1 refers to the flux tube and $\frac{3}{4}$ to the longitudinal part. (b) Graphs of $P_l(g)$, for $l = 1, \ldots, 20$. It can be seen that even for small values of l, $P_l(g)$ approaches 1 for a small g. (c) The one plaquette system we use in the demonstration.

where $\mathbf{n}$'s are the vertices of the lattice, $k = 1, 2$ are the lattice directions, whose corresponding unit vectors are $\hat{\mathbf{1}}$, $\hat{\mathbf{2}}$. For example, $L^k_{z\mathbf{n}}$ is the z component of the spin on the link emanating from the vertex $\mathbf{n}$ in the kth direction (the generalization to a 3D lattice is straightforward), and g is a constant. This should be compared to the Abelian Kogut-Susskind Hamiltonian [2,19] $H_{\mathrm{KS}} = \frac{g^2}{2}\sum_{\mathbf{n},k}(E^k_{\mathbf{n}})^2 - \frac{1}{g^2}\sum_{\mathbf{n}}\cos(\phi^1_{\mathbf{n}} + \phi^2_{\mathbf{n}+\hat{1}} - \phi^1_{\mathbf{n}+\hat{2}} - \phi^2_{\mathbf{n}})$. Unlike the Kogut-Susskind Hamiltonian, in our case we are dealing with 3D angular momentum operators. Nevertheless, for large values of l, the first quadratic term in the Hamiltonian coincides with the electric part of the Abelian Kogut-Susskind Hamiltonian, with the z components of the angular momentum playing the role of an electric field E, and the second, quartic part with the magnetic part of the Kogut-Susskind Hamiltonian. This can be seen qualitatively when considering the matrix elements of $|m| \ll l$, for which $\frac{L_+}{\sqrt{l(l+1)}}|l, m\rangle \approx |l, m \pm 1\rangle$, similar to $e^{\pm i\phi}|m\rangle = |m \pm 1\rangle$ in the Kogut-Susskind model. We shall test this equivalence quantitatively for the case of a single plaquette (Fig. 1).

For every l, the SG Hamiltonian manifests a local U(1) gauge symmetry, that is generated by the local operators (defined on the vertices of the lattice) $G_{\mathbf{n}} = \sum_k \triangle_k L^k_{z\mathbf{n}}$ (where $\triangle_k f_{\mathbf{n}} = f_{\mathbf{n}+\hat{\mathbf{k}}} - f_{\mathbf{n}}$) which commute with the Hamiltonian: for a given vertex, $G_{\mathbf{n}}$ trivially commutes with all the plaquettes which do not contain $\mathbf{n}$. As for the other four plaquettes, the commutation relation is zero, because $[L_z, L_\pm] = \pm L_\pm$. For example, $[G_{\mathbf{n}}, L^1_{+,\mathbf{n}}L^2_{+,\mathbf{n}+\hat{1}}L^1_{-,\mathbf{n}+\hat{2}}L^2_{-,\mathbf{n}}] = [L^1_{z\mathbf{n}} + L^2_{z\mathbf{n}}, L^1_{+,\mathbf{n}}L^2_{+,\mathbf{n}+\hat{1}}L^1_{-,\mathbf{n}+\hat{2}}L^2_{-,\mathbf{n}}] = L^1_{+,\mathbf{n}}L^2_{+,\mathbf{n}+\hat{1}}L^1_{-,\mathbf{n}+\hat{2}}L^2_{-,\mathbf{n}} - L^1_{+,\mathbf{n}}L^2_{+,\mathbf{n}+\hat{1}}L^1_{-,\mathbf{n}+\hat{2}}L^2_{-,\mathbf{n}} = 0$. Static external charges $|\{Q_{\mathbf{n}}\}\rangle$ are introduced to the system by fixing a subspace by the constraint $G_{\mathbf{n}}|\{Q_{\mathbf{n}}\}\rangle = Q_{\mathbf{n}}|\{Q_{\mathbf{n}}\}\rangle$.

In order to have something useful for simulations, we would like to have that $H_l \to H_{\mathrm{KS}}$ for large l's, sufficiently fast. Thus, we shall consider a comparison between the SG Hamiltonian with a constant l and a truncated version of the Kogut-Susskind Hamiltonian with $-l \le E \le l$. It is straightforward to see, using perturbation theory in g^{-1}, that in the strong limit of the Hamiltonian ($g \gg 1$), the ground states of the SG and Kogut-Susskind Hamiltonians coincide up to a certain order in the perturbative expansion, depending on l and the charge distribution. On the other hand, in the weak coupling limit, we shall examine the effect of truncation in a nonperturbative manner, for a single plaquette system.

Case of a single plaquette.—Consider a single plaquette with two opposite unit static charges in the lower vertices [see Fig. 1(c)]. Using the gauge invariance and Gauss's law, a possible gauge-invariant basis of states is $|m\rangle \equiv |m, m-1, 1-m, 1-m\rangle \quad (m = -l+1, \ldots, l)$ where these are the eigenvalues of the electric field on each link, from the lower one, counterclockwise. Relying upon the results of Drell *et al.* in Ref. [5], the ground state of this system, for weak coupling, is given by a Bloch-like wave function in the tight-binding limit $\chi(\theta) = \sum_{n=-\infty}^{\infty} e^{(in\pi/2)}e^{-1/4g^2(\theta-2\pi n)^2}$, where θ is the magnetic field in the plaquette. On the link connecting the charges, $\langle E_1\rangle = \frac{3}{4} + \frac{\pi}{g^4}(\frac{\pi^2-4}{2})e^{-\pi^2/2g^2}$. This can be understood as the contributions of two parts: One is the trivial contribution of the longitudinal, classical, static Coulomb field ($\frac{3}{4}$). The second part is much more interesting: it is nonanalytic in $g = 0$ and therefore it is nonperturbative in g. It is this type of mechanism that is responsible for confinement in the weak regime in large 2D spatial lattices. In Fig. 1(a), $\langle E_1\rangle$ is plotted as a function of g—both for the truncated Kogut-Susskind Hamiltonian and the SG Hamiltonian for several values of l, and the analytic result of Ref. [5] as well. For $g < 1$, the truncated and SG results coincide with each other and with the analytical approximation for $l \approx 2, 3$. For large values of g, the flux-tube value of 1 is reached already for $l = 1$.

In order to understand the effect of truncation, we expand this state in the m basis—$|\chi\rangle = \sum_{m=-\infty}^{\infty} a_m|m\rangle = \sum_{m=-\infty}^{\infty} e^{-g^2(m-3/4)^2}|m\rangle$, and take only $-l+1 \le m \le l$. As a measure of the accuracy of truncation, we calculate the probability to be in the truncated subspace: $P_l(g) = \frac{1}{\langle\chi|\chi\rangle}\sum_{m=-l+1}^{l}|a_m|^2$ as one can see in Fig. 1(b), this function approaches a value of 1 quickly even for small finite l's, which means that the truncated theory still shows the same effect for small g's.

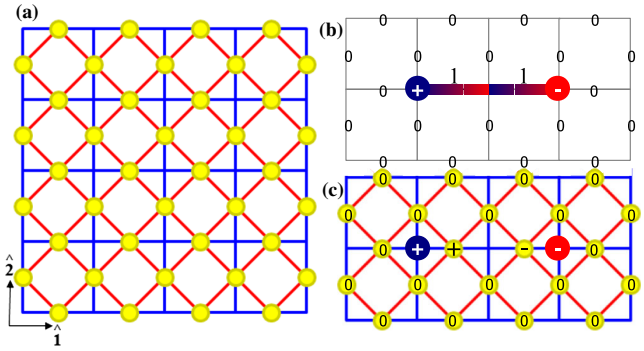

FIG. 2 (color online). (a) The simulation lattice. As explained in the text, the atoms (yellow circles) are aligned along the links of a 2D square lattice, with basis vectors $\hat{\mathbf{1}}$ and $\hat{\mathbf{2}}$. On the blue (horizontal/vertical) lines the tunneling rates between neighboring atoms are t^s_α [in Hamiltonian (2)], and on the red (diagonal) lines—t^d_α. In Hamiltonian (3), $z-z$ interaction is between nearest neighbors along both the red and blue lines, and $x-x$, $y-y$ interactions are only along the red ones. (b) The flux tube (zeroth order in perturbative expansion, in the strong limit of the Kogut-Susskind Hamiltonian) connecting two opposite charges. (c) The flux tube in the language of our simulating system.

Simulating the $l=1$ SG Hamiltonian.—Let us consider a 2D square optical lattice [21], whose minima coincide with the links of the square lattice of the SG Hamiltonian (the generalization to a 3D spatial lattice is straightforward). Each minimum is populated by a single atom of three different atomic levels, forming a $l=1$ spinor [see Fig. 2(a)]. We use it to develop an effective theory [22], which manifests confining flux tubes similar to the ones in CQED. We first turn to the derivation of an effective generalized spin-1 XXZ Hamiltonian on this lattice.

The Hamiltonian describing the dynamics of three atomic species $\alpha \in \{+,0,-\}$ on such an optical lattice contains same-species tunneling terms along the $\hat{\mathbf{1}}$, $\hat{\mathbf{2}}$ directions and the diagonal directions as well, and on-site spin and number dependent terms. A pictorial representation of the interactions can be found in Fig. 2(a), and a more detailed description of the lattice structure and the optical potential can be found in the Supplemental Material [23]. Generalizing from [20] we obtain the Hamiltonian:

$$\begin{aligned} H = &-\sum_{\mathbf{n},\alpha}(t^s_\alpha(a^\dagger_{\mathbf{n},\alpha}a_{\mathbf{n}+\hat{\mathbf{1}},\alpha} + b^\dagger_{\mathbf{n},\alpha}b_{\mathbf{n}+\hat{\mathbf{2}},\alpha}) + t^d_\alpha(a^\dagger_{\mathbf{n},\alpha}b_{\mathbf{n},\alpha} \\ &+ a^\dagger_{\mathbf{n},\alpha}b_{\mathbf{n}+\hat{\mathbf{1}},\alpha} + b^\dagger_{\mathbf{n},\alpha}a_{\mathbf{n}+\hat{\mathbf{2}},\alpha} + a^\dagger_{\mathbf{n}+\hat{\mathbf{2}},\alpha}b_{\mathbf{n}+\hat{\mathbf{1}},\alpha}) + \text{H.c.}) \\ &+ \sum_{\mathbf{n},k,\alpha}\Delta^k_{\mathbf{n},\alpha}N^k_{\mathbf{n},\alpha} + \frac{U_o}{2}\sum_{\mathbf{n},k}N^k_{\mathbf{n}}(N^k_{\mathbf{n}}-1) \\ &+ \frac{U_2}{2}\sum_{\mathbf{n},k}(\vec{S}^{k^2}_{\mathbf{n}} - 2N^k_{\mathbf{n}}), \end{aligned} \tag{2}$$

where for horizontal links the annihilation operators are $a_{\mathbf{n},\alpha}$, and the number operators are $N^1_{\mathbf{n},\alpha} = a^\dagger_{\mathbf{n},\alpha}a_{\mathbf{n},\alpha}$, and for vertical links $-b_{\mathbf{n},\alpha}$ and $N^2_{\mathbf{n},\alpha} = b^\dagger_{\mathbf{n},\alpha}b_{\mathbf{n},\alpha}$; $N^k_{\mathbf{n}} = \sum_\alpha N^k_{\mathbf{n},\alpha}$ and $\vec{S}^k_{\mathbf{n}}$ is the total on-site spin (see Ref. [20]).

We set the parameters $\Delta^k_{\mathbf{n},\pm} = \frac{\delta}{2} + 2\lambda + \mu \mp 2\lambda(q_{\mathbf{n}} + q_{\mathbf{n}+\hat{\mathbf{k}}})$, $\Delta_0 = 0$, with $\delta \ll U_0, U_2, \mu \ll \lambda \ll U_0, U_2$, and $q_{\mathbf{n}}$ being integer C numbers which will be later related to the static charges. We also introduce a new variable z, satisfying $U_2 = zU_0$.

Derivation of a generalized XXZ Hamiltonian.—The first effective calculation, which leads to a generalized XXZ model, is similar to the one in Ref. [20]. Because the U local terms are much larger than the others, it is reasonable to obtain, perturbatively, an effective Hamiltonian around them [22]. Unlike in Ref. [20], we do not include the small local terms $\sum_{\mathbf{n},k,\alpha}\Delta^k_{\mathbf{n},\alpha}N^k_{\mathbf{n},\alpha}$ in the constraining part of the Hamiltonian, but rather treat them as the first order contribution to the effective Hamiltonian. We divide that into two parts: one is the λ, μ, $q_{\mathbf{n}}$ dependent part, which we put aside at the moment; The other δ dependent part will be used to construct "two-site"connected local diagonal Hamiltonians: the energy contribution of this part from each link will be equally distributed among the six connections it has with other links (to which it is connected by tunneling).

The tunneling rates are chosen to be real: $t^s_+ = t^s_- = t^d_+ = t^d_- = \frac{1}{4}\sqrt{\frac{U_0(24\lambda-5\epsilon)(\epsilon+24\lambda)}{6\epsilon}}$, $t^s_0 = 0$, $t^d_0 = \Omega\sqrt{\frac{3U_0(24\lambda-5\epsilon)}{2\epsilon(\epsilon+24\lambda)}}$, where $\frac{\lambda^2}{U_0}, \frac{\Omega^2}{U_0} \ll \epsilon \ll \Omega \ll \lambda$ and $t^d_0 \ll t^d_\pm$. Finally, we set $\delta = -12\lambda - \epsilon$ and $z = \frac{1}{4} - \frac{6\lambda}{\epsilon}$. Then we can apply the effective calculation as in Ref. [20]. Collecting these results with the λ, μ, $q_{\mathbf{n}}$ dependent part, we get, up to a constant energy, the first effective Hamiltonian,

$$\begin{aligned} H^{(1)}_{\text{eff}} = &2\lambda\sum_{\text{str+diag}} L_{z,\mathbf{n}}L_{z,\mathbf{n}'} + \Omega\sum_{\text{diag}}(L_{x,\mathbf{n}}L_{x,\mathbf{n}'} + L_{y,\mathbf{n}}L_{y,\mathbf{n}'}) \\ &+ \sum_{\mathbf{n},k}((2\lambda+\mu)(L^k_{z,\mathbf{n}})^2 - 2\lambda(q_{\mathbf{n}} + q_{\mathbf{n}+\hat{\mathbf{k}}})L^k_{z,\mathbf{n}}) + O(\epsilon), \end{aligned} \tag{3}$$

where the $z-z$ interactions are between links that share a vertex and the $x-x$,$y-y$ only between links that share both a vertex and a plaquette [see Fig. 2(a)]. This is an example of a frustrated XXZ model Hamiltonian, which is of interest of its own. One can easily check that the scale hierarchy is not violated.

Imposing gauge invariance on the system.—In the second step, we employ the method of Ref. [18]. Define $c_{\mathbf{n}} \equiv \frac{1}{\sqrt{2}}L^1_{-\mathbf{n}}$, $d_{\mathbf{n}} \equiv \frac{1}{\sqrt{2}}L^2_{-\mathbf{n}}$, $G_{\mathbf{n}} \equiv L^1_{z,\mathbf{n}} + L^2_{z,\mathbf{n}} + L^1_{z,\mathbf{n}-\hat{\mathbf{1}}} + L^2_{z,\mathbf{n}-\hat{\mathbf{2}}}$, and rewrite the effective Hamiltonian as

$$\begin{aligned} H^{(1)}_{\text{eff}} = &\lambda\sum_{\mathbf{n}}(G_{\mathbf{n}} - q_{\mathbf{n}})^2 + \mu\sum_{\mathbf{n},k}(L^k_{z,\mathbf{n}})^2 \\ &+ 2\Omega\sum_{\text{diag}}(c^\dagger_{\mathbf{n}}d_{\mathbf{n}'} + \text{H.c.}) \equiv H_G + H_E + H_R, \end{aligned} \tag{4}$$

which is similar to the Hamiltonian obtained by us previously [18,24] and from which, due to the scale hierarchy $\lambda \gg \mu, \Omega$, we shall obtain an effective Hamiltonian as in

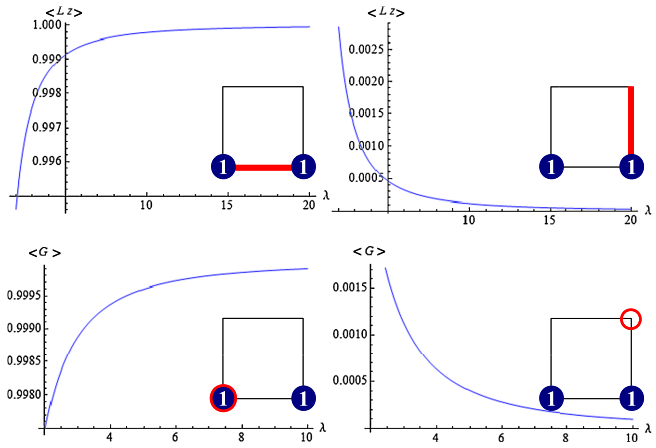

FIG. 3 (color online). An example of the emergence of gauge invariance in the second effective calculations for a single plaquette system ($l = 1$). Two unit charges are located in the lower vertices. The parameters are chosen such that for a large λ the system will be in the strong limit: $\mu = 1$, $\Omega = 0.1$. The expectation values of L_z along two links, as well as of the gauge transformation generators G at two vertices are plotted as a function of λ for the ground state. It can be seen that as λ grows, G converges to the local charges and hence Gauss's law and gauge invariance are introduced, and L_z approach the values of the lowest flux-tube state in the strong limit. Note the discussion on the signs in the text.

Ref. [18]. The constraint will be H_G (Gauss's law), and its ground sector contains the states of relevance for us. H_E commutes with it and hence becomes the first order of the effective Hamiltonian, and from H_R we get two contributions: one is the gauge-invariant plaquette term $H_B = -\frac{8\Omega^2}{\lambda}\sum_{m,n}(c^\dagger_{\mathbf{n}+\hat{\mathbf{2}}}d_{\mathbf{n}}c^\dagger_{\mathbf{n}}d_{\mathbf{n}+\hat{\mathbf{1}}} + \text{H.c.})$. The other one is due to the finiteness of the angular momentum representation matrices, but it is diagonal (and hence gauge invariant) and thus introduces a negligible first order correction to the energy but does not change the zeroth order ground state (the flux tube): $H'_B = -\frac{2\Omega^2}{\lambda}\sum_{\text{diag}}(|+\rangle\langle+| + |0\rangle\times\langle 0|)_{\mathbf{n}} \otimes (|0\rangle\langle 0| + |-\rangle\langle -|)_{\mathbf{n}'}$. Note that as $l \to \infty$ (in a truncated Kogut-Susskind theory), these terms approach identity matrices and act as an ignorable constant energy, and hence this term did not appear in the infinite case. An example for the emergence of gauge invariance as the constraint gets stronger is illustrated in Fig. 3.

Next we perform the change of variables [18]: $L^k_{z,\mathbf{n}} \to (-1)^{n_1+n_2}L^k_{z,\mathbf{n}}$, $\phi^k_{\mathbf{n}} \to (-1)^{n_1+n_2}\phi^k_{\mathbf{n}}$, and $Q_{\mathbf{n}} \equiv (-1)^{n_1+n_2}q_{\mathbf{n}}$ (which also swaps the $L_\pm$ operators on odd vertices). This change of signs is needed in order to get the correct signs for the Gauss's law constraint and the interactions of the SG Hamiltonian. Plugging it into the effective Hamiltonian we get

$$H^{(2)}_{\text{eff}} = \mu\sum_{\mathbf{n},k}(L^k_{z,\mathbf{n}})^2 + H_B + H'_B \tag{5}$$

and if we rescale the energy, using $\alpha = \frac{2}{g^2}\mu = \frac{16\Omega^2 g^2}{\lambda}$, we get that $\alpha^{-1}H^{(2)}_{\text{eff}}$ is the $l = 1$ SG Hamiltonian Eq. (1) plus the irrelevant term of $\alpha^{-1}H'_B$. Hence, because of the sign inversions between the SG and the simulating models, the manifestation of an electric flux tube between two confined static charges, to zeroth order, will be a line of alternating $+$, $-$ states of the atoms along the links connecting the two charges [see Fig. 2(c)]. Some specific suggestions for initial state preparation and possible measurements are presented in the Supplemental Material [23].

In this Letter, we have presented a new method to simulate CQED using ultracold atoms in optical lattices. We believe that this method may be experimentally accessible in the near future. Although we have constructed a realization of H_1, which allows for simulation of confinement around the strong coupling limit, the rapid convergence of H_l to the Kogut-Susskind model suggests an avenue towards the simulation of the nonperturbative effects of the weak coupling limit as well as phase transitions in $3 + 1$ dimensions. It would be intriguing to study the inclusion of dynamic matter fields in the model, which would lead to a full simulation of CQED.

The authors would like to thank L. Mazza for helpful discussions. B. R. acknowledges the support of the Israel Science Foundation, the German-Israeli Foundation, and the European Commission (PICC). I. C. is partially supported by the EU project AQUTE.

[1] K. G. Wilson, Phys. Rev. D **10**, 2445 (1974).
[2] J. Kogut and L. Susskind, Phys. Rev. D **11**, 395 (1975).
[3] A. M. Polyakov, Nucl. Phys. **B120**, 429 (1977).
[4] T. Banks, R. Myerson, and J. Kogut, Nucl. Phys. **B129**, 493 (1977).
[5] S. D. Drell, H. R. Quinn, B. Svetitsky, and M. Weinstein, Phys. Rev. D **19**, 619 (1979).
[6] S. Ben-Menahem, Phys. Rev. D **20**, 1923 (1979).
[7] J. I. Cirac and P. Zoller, Nature Phys. **8**, 264 (2012).
[8] J. I. Cirac, P. Maraner, and J. K. Pachos, Phys. Rev. Lett. **105**, 190403 (2010).
[9] A. Bermudez, L. Mazza, M. Rizzi, N. Goldman, M. Lewenstein, and M. A. Martin-Delgado, Phys. Rev. Lett. **105**, 190404 (2010).
[10] O. Boada, A. Celi, J. I. Latorre, and M. Lewenstein, New J. Phys. **13**, 035002 (2011).
[11] A. Retzker, J. I. Cirac, and B. Reznik, Phys. Rev. Lett. **94**, 050504 (2005).
[12] B. Horstmann, B. Reznik, S. Fagnocchi, and J. I. Cirac, Phys. Rev. Lett. **104**, 250403 (2010).
[13] O. Boada, A. Celi, J. I. Latorre, and M. Lewenstein, Phys. Rev. Lett. **108**, 133001 (2012).
[14] M. Hermele, M. P. A. Fisher, and L. Balents, Phys. Rev. B **69**, 064404 (2004).
[15] H. Weimer, M. Muller, I. Lesanovsky, P. Zoller, and H. P. Büchler, Nature Phys. **6**, 382 (2010).
[16] H. P. Büchler, M. Hermele, S. D. Huber, M. P. A. Fisher, and P. Zoller, Phys. Rev. Lett. **95**, 040402 (2005).

[17] S. Tewari, V. W. Scarola, T. Senthil, and S. Das Sarma, Phys. Rev. Lett. **97**, 200401 (2006).
[18] E. Zohar and B. Reznik, Phys. Rev. Lett. **107**, 275301 (2011).
[19] J. B. Kogut, Rev. Mod. Phys. **51**, 659 (1979).
[20] L. Mazza, M. Rizzi, M. Lewenstein, and J. I. Cirac, Phys. Rev. A **82**, 043629 (2010).
[21] M. Lewenstein, A. Sanpera, and V. Ahufinger, *Ultracold Atoms in Optical Lattices: Simulating Quantum Many-Body Systems* (Oxford University, New York, 2012).
[22] C. E. Soliverez, J. Phys. C **2**, 2161 (1969).
[23] See Supplemental Material at http://link.aps.org/supplemental/10.1103/PhysRevLett.109.125302 for more details about the optical potential and the superlattice needed, and about possible initial states preparation and measurement.
[24] The correspondence is to the Hamiltonians $H_0 + H_R$ in the second and fourth paragraphs of the third page of Ref. [18], as follows: $L_z \sim \delta$; $c, d \sim \tilde{a}, \tilde{b}$; $G - q \sim G$.